



# Reaction–complexation coupling between an enzyme and its polyelectrolytic substrate: Determination of the dissociation constant of the hyaluronidase–hyaluronan complex from the hyaluronidase substrate-dependence

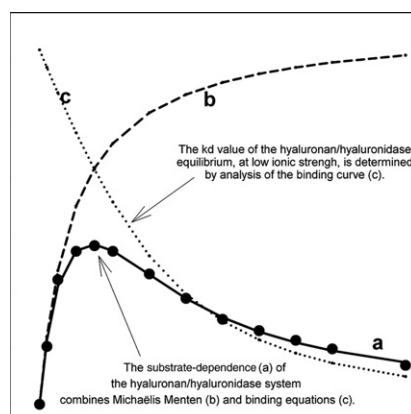
Hélène Lenormand <sup>\*</sup>, Fériel Amar-Bacoup <sup>1</sup>, Jean-Claude Vincent

Laboratoire "Polymères, Biopolymères, Surfaces", UMR 6270 CNRS – Université de Rouen, 76821 Mont-Saint-Aignan Cedex, France

## HIGHLIGHTS

- The hyaluronan/hyaluronidase system is a reaction–complexation coupling.
- The substrate-dependence combines Michaelis–Menten and binding equations.
- For the first time, the  $K_d$  value of the system at low ionic strength is determined.

## GRAPHICAL ABSTRACT



## ARTICLE INFO

### Article history:

Received 28 January 2013  
Received in revised form 25 February 2013  
Accepted 25 February 2013  
Available online 5 March 2013

### Keywords:

Hyaluronan  
Hyaluronidase  
Polysaccharide–protein complex  
Enzyme activity  
Determination of dissociation constant  
Modeling

## ABSTRACT

Hyaluronan (HA) is catalytically hydrolyzed by hyaluronidase (HAase). Depending on pH, HA is able to form a non-productive electrostatic complex with HAase in addition to the classical enzyme–substrate complex. Experiments have shown the strong inhibition of the HA hydrolysis catalyzed by HAase when performed at high HA over HAase concentration ratio and low ionic strength. The substrate-dependence thus shows a non-classic inhibition of HAase at high substrate concentrations due to the sequestration of HAase by HA in the electrostatic complex. The modeling of the HA/HAase system is characteristic of a reaction–complexation coupling and it is very difficult to study reaction or binding, separately. Here, we have established the equation controlling the global system and shown that the substrate-dependence of such a system is a direct combination of a pure Michaelis–Menten equation associated with the reaction and a hyperbolic curve associated with the binding. At low substrate concentrations, the hyperbola, representing the relative part of HAase not sequestered by HA, can be assimilated to a straight line. We have established the relationship between the slope of that straight line and the dissociation constant of the electrostatic HA–HAase complex.

<sup>\*</sup> Corresponding author at: ESITPA, 3 rue du tronquet, CS 40118, 76134 Mont Saint Aignan Cedex. Tel.: +33 2 32 82 91 76.  
E-mail address: [helene.lenormand@univ-rouen.fr](mailto:helene.lenormand@univ-rouen.fr) (H. Lenormand).

<sup>1</sup> Present address: ESITPA, 3 rue du tronquet, CS 40118, 76134 Mont Saint Aignan Cedex.

Fitting the theoretical equation to the experimental data allowed us to determine, for the first time, the  $K_d$  value of the non-productive HA–HAase complex at low ionic strength.

© 2013 Published by Elsevier B.V.

## 1. Introduction

Interactions between two biomacromolecules occur according to two main classes of mechanisms: non-compatibility between the two biomacromolecules leading to thermodynamic segregation, or electrostatic interactions leading to complex coacervation [1]. Enzymes belong to the protein family and thus are polyelectrolytes either negatively or positively charged, depending on pH. Such enzymes can form electrostatic complexes with oppositely charged polyelectrolytes. Protein–polyelectrolyte coacervates [1,2] have essentially been used in micro-encapsulation [3] and protein purification [4,5]. Polysaccharides constitute an important class of biological polyelectrolytes and are most often negatively charged. Moreover, proteins and polysaccharides have an important role in organization and functioning of living cells and it is likely that coacervation is involved in the regulation of enzyme activities in the extracellular matrix (ECM) which contains high concentrations of both charged polysaccharides and proteins.

Hyaluronidase (HAase) is one of these enzymes. It is involved in several fundamental biological phenomena, such as fertilization and cancer [6]. Its natural substrate is hyaluronan (HA) which is hydrolyzed into HA oligosaccharides. HA is a linear high-molar-mass polysaccharide composed of D-glucuronic acid- $\beta$ (1,3)-N-acetyl-D-glucosamine disaccharide units linked together through  $\beta$ (1,4) glycosidic bonds. It is thus a negatively charged polysaccharide. HA is a major constituent of the ECM of vertebrates and is involved in many biological processes, such as cellular adhesion, mobility and differentiation processes [6–11]. Moreover, its properties are a function of its chain length. As HA oligosaccharides (4 to 25 disaccharides) have an angiogenic action [11–13] contrary to native HA [14], the balance between high molecular weight HA and low molecular weight HA plays a role in cancer development [15,16].

In vitro, at neutral or acidic pH and low ionic strength, HA is able to form electrostatic complexes with positively charged proteins such as bovine serum albumin (BSA) [17–22] or lysozyme (LYS) [21–24], but also with HAase [18,20,21,25]. In a pure HA/HAase mixture, we have shown that: i) when HAase is in excess, all the HA molecules are complexed by HAase and are still hydrolyzable by the excess of HAase (free HAase), and ii) when HA is in excess, all the HAase molecules are complexed by HA and are no longer able to catalyze the HA hydrolysis. This produces an inhibition of the HA hydrolysis reaction by high substrate concentrations, because of the complete sequestration of the enzyme at high HA concentrations [26]. This constitutes a non-classic inhibition by excess of substrate according to a mechanism very different from the classic one used in enzymology: there is no specific inhibitory site on the enzyme surface and the classical kinetic equations with competitive or uncompetitive mechanisms are not valid. Moreover, this inhibition can be reversed by adding other proteins able to form electrostatic complexes with HA. Maingonnat and al. [27] have shown that not only BSA, but also immunoglobulins, hyaluronectin and hemoglobin are able to enhance the HAase activity at pH 4. We have shown that BSA and LYS are able to modulate the HAase activity over a wide pH domain ranging from pH 3 to pH 9 [21]. We have also shown that the increase in HAase activity is not an activation of the enzyme, but rather the abolishment of the HAase inhibition due to the electrostatic complex formed between HA and HAase. There is a competition between proteins and HAase in forming the electrostatic complex with HA. This process is non-specific in the sense that it involves various proteins and non-specific electrostatic interactions. Nevertheless, it depends on the protein because the increase in HAase

activity requires a positive competition between the protein and HAase to form the complex. In other words, the dissociation constant of the electrostatic HA–protein complex has to be lower than the dissociation constant of the electrostatic HA–HAase complex. This has been modeled [26] and we have shown that the present condition, together with the two previously stated assumptions (the HAase molecules sequestered by HA are not catalytically active, and the HA molecules complexed with HAase are still potentially hydrolyzable) are sufficient to obtain the different behaviors observed with the HA–HAase–protein system.

As HA is a very important ECM component, it interacts with numerous cell receptors, and its affinity for these proteins has been studied. The dissociation constant for the CD44–HA association has been estimated to  $5 \cdot 10^{-6}$  M by Skelton et al. [28]. The binding constant for the HA sulfate–fibroblast growth factor association has been estimated at  $1.36 \cdot 10^8$  M $^{-1}$  by Freeman et al. [29]. However, the nature of the interactions involved in the binding is not always clearly defined. For example, what is the significance of a specific binding? Is an optimal electrostatic binding, a specific binding? In some other cases, the electrostatic nature of the binding is more evident, for example because of the effect of the ionic strength on the binding. The binding of HA on hepatocytes has been estimated at  $10^{-7}$  M by Frost et al. [30], this binding decreasing when the ionic strength is increased and increasing when the ionic strength is decreased. Only a few dissociation constants of pure electrostatic complexes formed between HA and various proteins are known. The only known constant concerns HA–LYS complexes which has been estimated at  $10^{-7}$ – $10^{-8}$  M by Van Damme et al. [23]. LYS is an enzyme, but HA is not a substrate of LYS and the binding is non-productive. The problem is much more complicated with HAase which is the natural enzyme degrading HA. It means that in the case of HAase, two complexes exist, the non-productive electrostatic HA–HAase complex and the specific catalytic HA–HAase complex based on electrostatic, hydrophobic and Van der Waals interactions. It means that mixing HA with HAase at a temperature close to 37 °C induces the HA hydrolysis reaction which modifies the HA molecule. The system is thus continuously changing and it is not possible to observe the binding phenomenon at this temperature by avoiding the reaction phenomenon. The determination of the dissociation constant of the electrostatic HA–HAase complex is thus very difficult. Two possibilities are offered to us: i) performing the binding measurements at low temperature to slow down the reaction, but the constant is not representative of the temperature of the catalytic action, or ii) estimating the binding parameters from the hydrolysis kinetics which is modified by the binding–reaction coupling.

In the present paper, we demonstrate that we can use the global substrate-dependence of the HA–HAase system at 37 °C to determine the values of the Michaelis–Menten constants of HAase and the dissociation constant of the electrostatic HA–HAase complex.

## 2. Theory

### 2.1. The kinetic equation

From the kinetic point of view, the classical behavior of an enzyme reaction has been described by the Michaelis–Menten model in 1913. The initial reaction rate,  $V_i$ , is proportional to the total enzyme concentration and is a hyperbolic function of the substrate concentration:

$$V_i = k \times [E]_t \times [S]/(K_m + [S]) \quad (1)$$

where  $k$  is the limiting rate constant,  $K_m$  the Michaelis constant,  $[S]$  the substrate concentration and  $[E]_t$  the total concentration of the active enzyme catalyzing the reaction.

In the presence of a charged polymeric substrate such as HA, depending on the ionic strength, electrostatic interactions exist between HA and HAase, and HA–HAase complexes are formed. It has been shown [20,31] that i) this complex is a potential substrate for the free soluble HAase and ii) the complexed HAase is not catalytically active. At high ionic strength, the electric charges borne by the two macromolecules, HA and HAase, are screened by the numerous small ions in solution and almost all the enzyme molecules are free and active. Conversely, at low ionic strength, HA–HAase electrostatic complexes are formed in which one HAase molecule interacts with an HA fragment of  $n$  disaccharides,  $HA_n$ . At pH 4 and without any added salt,  $n$  equals 57 [25].

Because a) the kinetics of the HA hydrolysis catalyzed by HAase is a first order kinetics [31], the kinetics does not show any induction period [31], and c) the exchange between HAase and a competitive protein (BSA) in the formation of the electrostatic complex is instantaneous [19], we may consider that the HA/HAase binding is a rapid equilibrium which can be described by the following equations:



where  $HAase_a$  is the free and active HAase and  $HA_n-HAase$  the complex composed of an HA fragment and a non active bound HAase molecule. The complex is characterized by its dissociation constant  $K_d$ :

$$K_d = [HA_n] \cdot [HAase_a] / [HA_n-HAase] \quad (3)$$

and the mass conservation laws give:

$$[HAase_a] + [HA_n-HAase] = [HAase]_0 \quad (4)$$

$$[HA_n] + [HA_n-HAase] = [HA_n]_0 \quad (5)$$

where  $[HA_n]_0$  is the total concentration of HA fragments containing  $n$  carboxyl groups (i.e. containing  $n$  disaccharides of 401 g.mol<sup>-1</sup> M mass) and  $[HAase]_0$  the total HAase concentration, the molar mass of HAase being 57,000 g.mol<sup>-1</sup>.  $[HA_n-HAase]$  is the concentration of the bound HAase,  $[HAase_a]$  is the concentration of the free and active enzyme. The total concentrations are given by:

$$[HA_n]_0 = [HA]_0 (\text{in g.L}^{-1}) / (401 \times n) \quad (6)$$

$$[HAase]_0 = [HAase]_0 (\text{in g.L}^{-1}) / 57000 \quad (7)$$

where  $[HA]_0$  is the total hyaluronan concentration.

Solving the equation system (Eqs. (3), (4), (5)) leads to the second degree equation [32]:

$$[HAase_a]^2 + [HAase_a]([HA_n]_0 + K_d - [HAase]_0) - K_d[HAase]_0 = 0 \quad (8)$$

which has two solutions of opposite sign; the positive solution thus gives the concentration of the free and active HAase. As only the free HAase molecules are active, this concentration corresponds to the total concentration of the active HAase, i.e.  $[E]_t$  in Eq. (1):

$$[HAase_a] = \left[ -([HA_n]_0 + K_d - [HAase]_0) + \sqrt{([HA_n]_0 + K_d - [HAase]_0)^2 + 4K_d \times [HAase]_0} \right] / 2. \quad (9)$$

The initial hydrolysis rate is thus given by the expression:

$$V_i = k \times [HAase_a] \times [HA_\beta]_0 / (K_m + [HA_\beta]_0) \quad (10)$$

where  $[HA_\beta]_0$  is the initial substrate concentration, equal to the concentration of the potentially cleavable  $\beta(1,4)$  bonds of HA [31]:  $[HA_\beta]_0 = n \times [HA_n]_0$ .

## 2.2. The substrate-dependence of HAase and its two contributions

$V_i$  can also be expressed as:

$$V_i = \frac{[HAase_a]}{[HAase]_0} \times V_m \times [HA_\beta]_0 / (K_m + [HA_\beta]_0) \quad (11)$$

where  $V_m = k \times [HAase]_0$ , according to the classic enzyme kinetic laws.  $V_m \times [HA_\beta]_0 / (K_m + [HA_\beta]_0)$  is thus the reaction contribution, i.e. the Michaelis–Menten contribution to the hydrolysis rate and  $[HAase_a]/[HAase]_0$  the binding contribution, i.e. the contribution of the electrostatic HA–HAase complex formation.

The variations of  $V_i$  with respect to  $[HA_\beta]_0$  are called the substrate-dependence of the HA hydrolysis catalyzed by HAase. Our description suggests that the substrate-dependence of the HAase activity, when HAase forms electrostatic complexes with its substrate HA, can be described by Eq. (11) in which  $[HAase_a]$  is calculated by Eq. (9).

The theoretical substrate-dependences of the HAase activity were calculated from these two equations, by using two arbitrary fixed constants,  $V_m$  and  $K_m$  ( $V_m = 10^{-2}$  mol.L<sup>-1</sup>.s<sup>-1</sup> and  $K_m = 10^{-3}$  mol.L<sup>-1</sup>) and different values of the HA–HAase complex dissociation constant  $K_d$  ranging from  $10^{-1}$  to  $10^{-9}$  mol.L<sup>-1</sup>. Fig. 1 shows the different substrate-dependence curves obtained in the presence of binding for the different  $K_d$  values (curves a to i). It shows that the inhibitory effect of high substrate concentrations increases when the dissociation constant  $K_d$  is decreased. This corresponds to an increase in the bound part of HAase. Conversely, the inhibitory effect of high substrate concentrations decreases when the dissociation constant  $K_d$  is increased. A  $K_d$  constant equal to or lower than  $10^{-7}$  mol.L<sup>-1</sup> leads to a highly complexed system. Conversely, a  $K_d$  constant equal to or higher than  $10^{-3}$  mol.L<sup>-1</sup> leads to a non complexed system.

In addition, Eq. (11) allows us to calculate the two contributions to the global substrate-dependence: i) the reaction contribution does not depend on  $K_d$  and is represented by a unique curve whatever the  $K_d$  value (Fig. 2), this is the Michaelis–Menten curve (curve M) and ii) the binding contribution to the global substrate-dependence

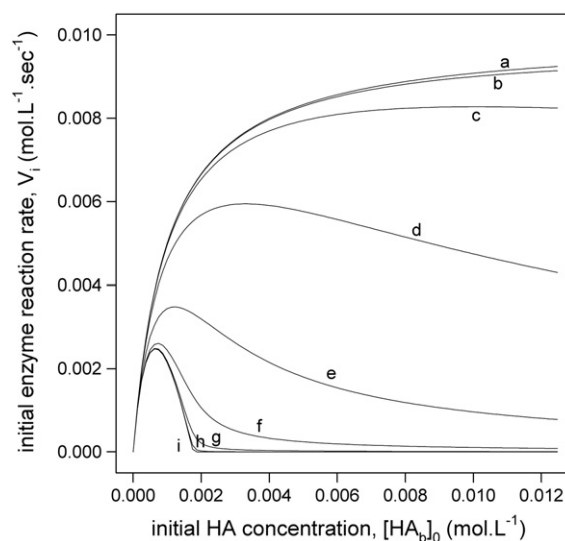


**Fig. 1.** Superimposition of the *in silico* substrate-dependences of the HAase activity calculated according to Eq. (11): HAase activity plotted as a function of the HA concentration for different values of the binding dissociation constant  $K_d$ : curve a ( $10^{-1}$  mol.L<sup>-1</sup>), b ( $10^{-2}$  mol.L<sup>-1</sup>), c ( $10^{-3}$  mol.L<sup>-1</sup>), d ( $10^{-4}$  mol.L<sup>-1</sup>), e ( $10^{-5}$  mol.L<sup>-1</sup>), f ( $10^{-6}$  mol.L<sup>-1</sup>), g ( $10^{-7}$  mol.L<sup>-1</sup>), h ( $10^{-8}$  mol.L<sup>-1</sup>), i ( $10^{-9}$  mol.L<sup>-1</sup>). Computational conditions were:  $V_m = 10^{-2}$  mol.L<sup>-1</sup>.s<sup>-1</sup>,  $K_m = 10^{-3}$  mol.L<sup>-1</sup> and  $[HA]_0$  ranging from 0 to 5 g.L<sup>-1</sup>.

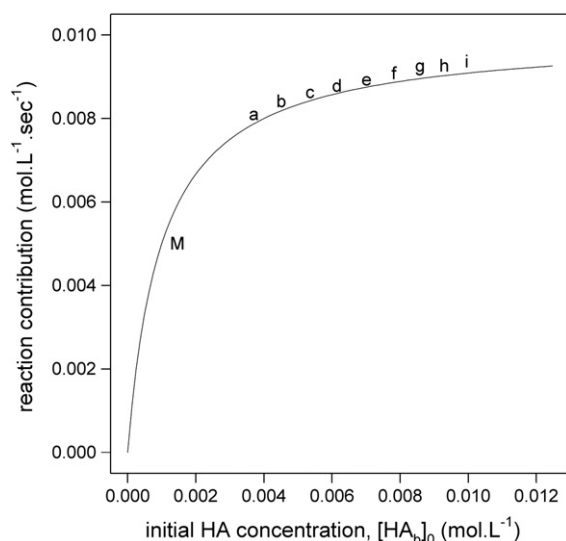


**Fig. 2.** Superimposition of the in silico reaction contribution to the global substrate-dependence (last terms of Eq. (11)) plotted as a function of the HA concentration for different values of the binding dissociation constant  $K_d$ : curve a ( $10^{-1}$  mol.L $^{-1}$ ), b ( $10^{-2}$  mol.L $^{-1}$ ), c ( $10^{-3}$  mol.L $^{-1}$ ), d ( $10^{-4}$  mol.L $^{-1}$ ), e ( $10^{-5}$  mol.L $^{-1}$ ), f ( $10^{-6}$  mol.L $^{-1}$ ), g ( $10^{-7}$  mol.L $^{-1}$ ), h ( $10^{-8}$  mol.L $^{-1}$ ), i ( $10^{-9}$  mol.L $^{-1}$ ). Computational conditions were those used in Fig. 1. The curve does not depend on  $K_d$ . It is unique and corresponds to the Michaelis-Menten curve M.

which depends on the  $K_d$  values used in the calculations. Fig. 3 shows those binding contributions obtained for different  $K_d$  values (curves a to i). The major observation is that the binding contribution draws a straight line as a function of the HA concentration when the dissociation constant  $K_d$  is low ( $K_d < 10^{-7}$  M, curves g to i). When the dissociation constant is increased, the binding contribution draws a hyperbolic curve which can be approximated by a straight line at low HA concentrations. In all cases, the slope of the straight line depends on the  $K_d$  values.

The theoretical binding contributions plotted in Fig. 3 for different  $K_d$  values were then analyzed by measuring their slope in the region of low substrate concentrations (noted  $s$ ). Fig. 4 represents the slope

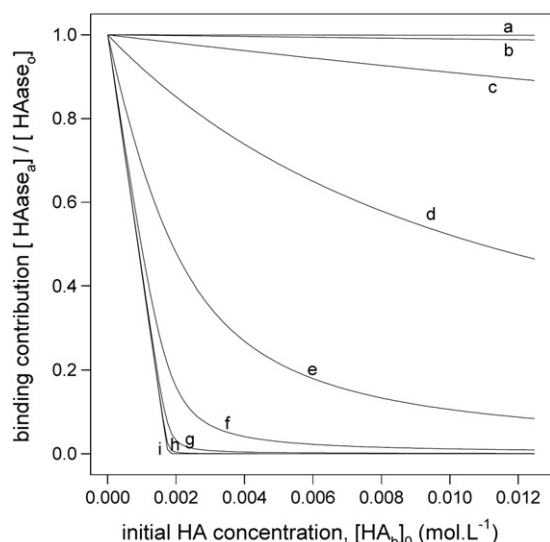


**Fig. 3.** Superimposition of the in silico binding contribution to the global substrate-dependence (first term of Eq. (11)) plotted as a function of the HA concentration for different values of the binding dissociation constant  $K_d$ : curve a ( $10^{-1}$  mol.L $^{-1}$ ), b ( $10^{-2}$  mol.L $^{-1}$ ), c ( $10^{-3}$  mol.L $^{-1}$ ), d ( $10^{-4}$  mol.L $^{-1}$ ), e ( $10^{-5}$  mol.L $^{-1}$ ), f ( $10^{-6}$  mol.L $^{-1}$ ), g ( $10^{-7}$  mol.L $^{-1}$ ), h ( $10^{-8}$  mol.L $^{-1}$ ), i ( $10^{-9}$  mol.L $^{-1}$ ). Computational conditions were those used in Fig. 1. At low HA concentrations, the slope of the binding contribution depends on  $K_d$ .

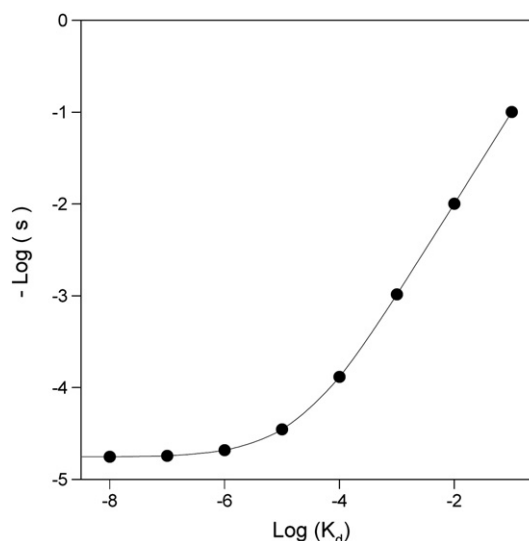


**Fig. 4.** The in silico slope of the binding contribution measured in Fig. 3 at low HA concentrations as a function of the value of the binding dissociation constant  $K_d$  in a Log-Log representation.

of the binding contribution obtained at low HA concentrations as a function of the dissociation constant  $K_d$  (in a Log-Log representation). The first conclusion is that, at low HA concentrations, the substrate-dependence of the HAase activity is definitely a direct combination of a Michaelis-Menten type curve with a straight line characterized by a slope which depends on the  $K_d$  value.

A more careful examination of the binding contribution curve should thus give quantitative information about the HAase complexation, such as the dissociation constant of the complex. Considering that i) the  $[HAase_a]/[HAase]_0$  ratio equals 1 when the HA concentration is null, and ii) the slope  $s$  of the  $[HAase_a]/[HAase]_0 = f([HA_b]_0)$  curve depends on the  $K_d$  value, it would be interesting to mathematically express the  $[HAase_a]/[HAase]_0$  ratio as a function of the  $K_d$  value, at low HA concentrations. The calculations, detailed in the Annex 1, lead to:

$$[HAase_a]/[HAase]_0 = 1 - [HA_n]_0 / (K_d + [HAase]_0) \quad (12)$$

the slope  $s$  of the binding contribution can thus be expressed by:

$$s = -1/n / (K_d + [HAase]_0) \quad (13)$$

and the global substrate dependence by:

$$V_i = [1 - s/n \times [HA_b]_0 \times V_m \times [HA_b]_0 / (K_m + [HA_b]_0)] \quad (14)$$

The  $K_d$  value was then calculated from Eq. (13):

$$K_d = -1/ns - [HAase]_0 \quad (15)$$

The first parts of the substrate-dependence curves (Fig. 1) were fitted to Eq. (14) by using the curve-fit program integrated in the SigmaPlot 2 software in order to estimate  $V_m$ ,  $K_m$  and  $s$ . The  $K_d$  values were then calculated from Eq. (15). This constitutes the “straight line fitting method”. Fig. 5 represents the calculated  $K_d$  values plotted as a function of the theoretical  $K_d$  values previously introduced in the model. We may observe an actual relationship between these two values; this suggests that the value of the dissociation constant of the HA-HAase complex is actually accessible by this procedure. However, a close relationship only exists when the  $K_d$  values are higher than  $10^{-4}$  mol.L $^{-1}$ . This is due to the relative level of  $[HAase]_0$  with respect to  $K_d$  in Eq. (13). When  $K_d$  is much lower than  $[HAase]_0$ , the



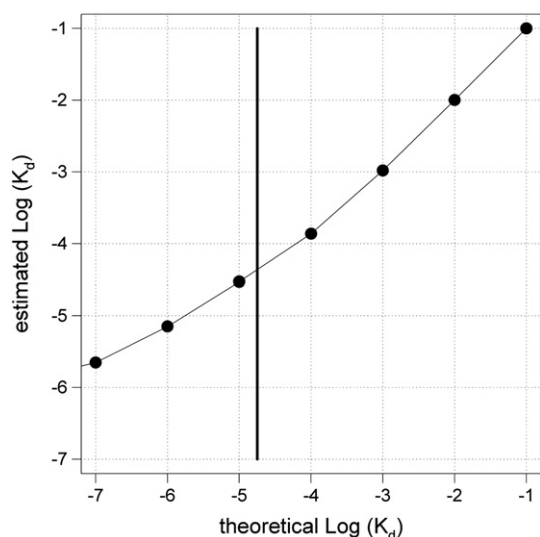


**Fig. 5.** The  $K_d$  values estimated by fitting the initial reaction rates of Fig. 1 to Eq. (14), by using the “straight line fitting method” are plotted as a function of the  $K_d$  values introduced in the *in silico* model.

slope is controlled by  $[HAase]_0$  and  $K_d$  cannot be precisely determined by the procedure. It is thus necessary to use the non-simplified equation system characterized by Eq. (11) in which  $[HAase]_a$  is given by Eq. (9). This constitutes the “global fitting method” which allows the direct estimation of  $V_m$ ,  $K_m$  and  $K_d$ .

### 3. Application to the experimental determination of the $K_d$ value of the HA–HAase complex from the HAase substrate-dependence

#### 3.1. Experimental procedures

Three types of HAase are distinguished according to their reaction mechanism [33]: glucuronidase, N-acetyl-glucosaminidase and bacterial lyase. Human HAases belong to the N-acetylglucosaminidase type and cleave HA at the  $\beta(1,4)$  glycosidic bond. Bovine testicular HAase (BTHAase) is also of the N-acetylglucosaminidase type [33] and can be considered as a model for the human HAases. BTHAase with a specific activity of 990 units/mg was obtained from Sigma (H 3884, lot 76 K8025,  $M_w = 57,000$  g). pI of BTHAase is between 5.3 and 6 [25]. Sodium hyaluronate from human umbilical cord with an estimated average molecular mass of  $0.967 \cdot 10^6$  g.mol $^{-1}$  was purchased from Sigma (H 1876, lot 127H0482). HA and BTHAase were used without any further purification. The HA mother solution (weighed as 10 g.L $^{-1}$ ) was prepared in milli-Q water and stored at  $-20$  °C. Since the activity of frozen BTHAase solutions did not remain constant, solutions freshly prepared by dissolving HAase in water buffer were used.

An aliquot of the HA mother solution was placed in a reactor, diluted to the desired concentration with Milli-Q water, adjusted to the desired pH with HCl (or KOH), stirred and maintained at 37 °C. After 2 min, the reaction was started by adding an adequate volume of a concentrated pH-adjusted HAase solution (10 g.L $^{-1}$ ). At each time point, an aliquot of the mixture was removed to the reactor and assayed by using the N-acetyl-D-glucosamine reducing ends assay. For each kinetics, the hydrolysis reaction was followed for 3 h and the concentration of the HA reducing ends was plotted against time. Measurement of the concentration of N-acetyl-D-glucosamine reducing ends enabled the determination of the HA chain concentration. It was performed according to the method described by Reissig et al. [34]. Because of the presence of proteins in the samples, turbidity and color were simultaneously present and we used the improvement of the Reissig method described in our previous papers [31,35].

The kinetic curve was obtained by plotting that concentration as a function of time, and the initial reaction rate was then determined by measuring the slope of that curve at time zero. This procedure was repeated for different initial HA concentrations varying from 0 to 0.012 mol.L $^{-1}$ . Finally, the substrate-dependence of BTHAase was obtained by plotting the initial hydrolysis rate as a function of the different initial substrate concentrations.

The substrate-dependence of BTHAase was experimentally obtained [36] with native HA, at 37 °C, pH 5 and very low ionic strength (no added salt) for an BTHAase concentration of 4 g.L $^{-1}$  (Fig. 6). This situation clearly enhances the electrostatic interactions between BTHAase and its substrate [20,31,32].

#### 3.2. Determination of the $K_d$ value of the HA–BTHAase complex

In a first step, we used the “straight line fitting method”. The first part of the substrate-dependence, i.e. the initial hydrolysis rate as a function of the initial  $\beta(1,4)$  site concentration ( $[HA]_0$ ), was fitted to Eq. (14) by using the “Curve fit program” integrated in the SigmaPlot 2 software. The Curve fit program allowed us to determine the estimated values for  $V_m$ ,  $K_m$  and  $s$ .  $K_d$  was then calculated by using Eq. (15). The fitting was performed by considering the first nine experimental points. The estimated values were then introduced in Eqs. (11) and (9) to rebuild the global substrate-dependence curve. It clearly appears that the curve obtained (curve a) does not agree with the experimental points. The main problem was that these first nine points did not exactly correspond to the conditions defined in our hypotheses, i.e., an  $[HAase]_a/[HAase]_0$  ratio close to 1. Diminishing the number of experimental points taken into account should thus improve this correspondence. Two additional fittings were thus performed by considering seven (curve b), then six (curve c), experimental points. Results are shown in Table 1. The conclusion is that i) the agreement with the experimental curve increases, ii) the estimated values of  $V_m$  and  $K_m$  increased, and iii) the estimated values of  $K_d$  decreased, when the number of experimental points was decreased.

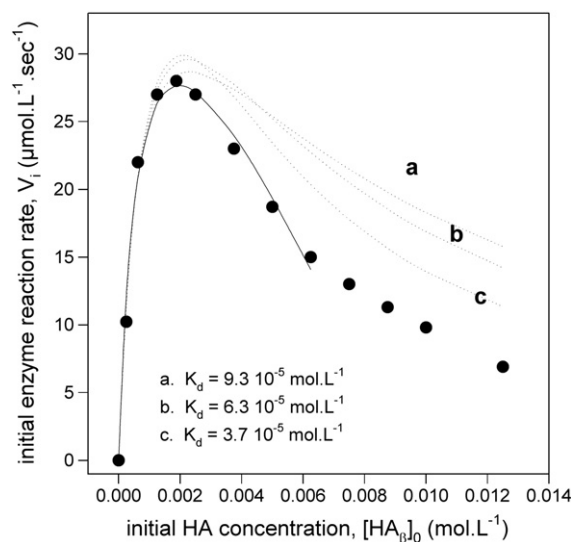


**Fig. 6.** Theoretical analysis of the experimental substrate-dependence of the HAase activity by using the “straight line fitting method”. The dark circles (●) represent the experimental initial rates plotted against the HA concentration. The reaction and binding parameters were then estimated by fitting the first part of the substrate-dependence to Eq. (14), by using the “straight line fitting method”. Three estimations were performed by considering the nine (a), then the seven (b) and finally the six (c) first experimental points. The estimated values of  $V_m$ ,  $K_m$  and  $K_d$  are summarized in Table 1. These values were introduced in Eqs. (11) and (9) to rebuild the global substrate-dependence curves: curve a for nine points, curve b for seven points and curve c for six points. The experimental conditions used were:  $10^6$  g.mol $^{-1}$  native HA substrate, 4 g.L $^{-1}$  HAase concentration, 37 °C, pH 5.

**Table 1**

Theoretical analysis of the experimental substrate-dependence of the HAase activity with  $10^6$  g.mol<sup>-1</sup> HA substrate at low ionic strength, 37 °C and pH 5. The HAase concentration was 4 g.L<sup>-1</sup>. The table gives the calculated reaction and binding parameters  $V_m$ ,  $K_m$  and  $K_d$ . In the first column, the nine first experimental points of Fig. 6 were fitted to Eq. (14) by using the “straight line fitting method”. The “Curve fit program” integrated in the SigmaPlot 2 software was used. The fitting gave the estimated values for  $V_m$ ,  $K_m$  and the slope  $s$ .  $K_d$  was then calculated by using Eq. (15). In the second column, the seven first experimental points were considered, and in the third column, only the first six experimental points were considered. The last column gives the values estimated by using the “global fitting program”.

	Straight line fitting with 9 experimental points	Straight line fitting with 7 experimental points	Straight line fitting with 6 experimental points	Global fitting
$V_m$	47.7	55.9	65.9	67.2
$K_m$	$7.1e-4$	$9.2e-4$	$1.1e-3$	$1.1e-3$
$K_d$	$9.3e-5$	$6.3e-5$	$3.7e-5$	$2.1e-5$

In a second step, we used the “global fitting program”. The global substrate-dependence was fitted to Eq. (11), completed by Eq. (9), by using the “Curve fit program” integrated in the SigmaPlot 2 software. In this case, the Curve fit program allowed us to directly determine the estimated values for  $V_m$ ,  $K_m$  and  $K_d$ . Results were added in Table 1. The fitting according to the “global fitting program” is now excellent (Fig. 7). The two contributions can now be easily distinguished, calculated according to Eq. (11) and plotted (Fig. 7). Table 1 clearly shows that the two fitting methods are in agreement with each other and that the estimated values obtained by the “straight line fitting method” tend to the estimated values obtained by the “global fitting method” when the number of experimental points considered by the first method was decreased.

The conclusion is that a good estimation of the different parameters controlling the experimental HA/BTHAase system was obtained:  $V_m = 67$  mol.L<sup>-1</sup>.s<sup>-1</sup>,  $K_m = 1.15 \cdot 10^{-3}$  mol.L<sup>-1</sup> and  $K_d = 2.2 \cdot 10^{-5}$  mol.L<sup>-1</sup>.

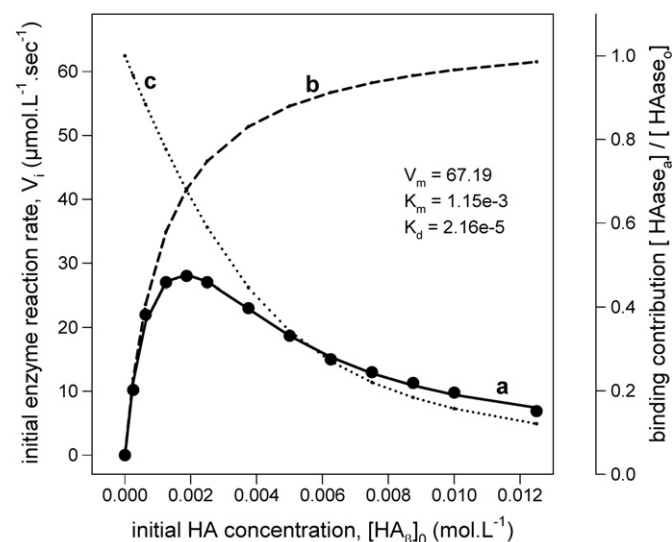


**Fig. 7.** Theoretical analysis of the experimental substrate-dependence of the HAase activity by using the “global fitting method”. The dark circles (●) represent the experimental initial rates plotted against the HA concentration. The reaction and binding parameters were estimated by fitting the substrate-dependence to Eqs. (11) and (9), by using the “global fitting method”. The estimated values of  $V_m$ ,  $K_m$  and  $K_d$  were then used to rebuild the global modeled substrate-dependence curve (full line a) according to Eq. (11), together with its reaction (dashed line b) and binding (dashed line c) contributions. The experimental conditions used were:  $10^6$  g.mol<sup>-1</sup> native HA substrate, 4 g.L<sup>-1</sup> HAase concentration, 37 °C, pH 5.

#### 4. Discussion and conclusion

The modeling of the HA/HAase system is characteristic of a complexation–reaction coupling where the reaction kinetics is controlled by the binding phenomenon and it is thus very difficult to study reaction and binding, separately. We have modeled the global system [26,32] and have shown here that the substrate-dependence of such a system is a direct combination of a pure Michaelis–Menten equation associated with the reaction and a hyperbola associated with the binding. The hyperbola associated with the binding represents the relative part of HAase which is not electrostatically sequestered by HA. We have also shown that the binding contribution can be related to the dissociation constant of the electrostatic HA–HAase complex.

In a second step, we have shown that the binding contribution can be modeled by a straight line at low HA concentrations and have established the relationship between the slope of the straight line and the dissociation constant  $K_d$  of the electrostatic HA–HAase complex. The application of this relationship to mathematically constructed substrate-dependences leads to a good estimation of the pre-defined dissociation constants of the electrostatic HA–HAase complex. This validates the fitting method using Eq. (14), called “straight line fitting method”. Nevertheless, the estimation of the  $K_d$  constant is possible only when the enzyme concentration is lower than  $K_d$ . Moreover, obtaining such a simple relationship has required simplifications requiring a reasonable set of data at low HA concentrations. This may cause difficulties for experimental substrate-dependence curves which may have a too restricted number of experimental points to determine the  $K_d$  constant. In the general case, the “global fitting method” using Eq. (11) will thus be used to determine the  $K_d$  constant. The two fitting methods used the curve-fit program integrated in the SigmaPlot 2 software which is based on the Levenberg–Marquardt algorithm [37]. The Levenberg–Marquardt algorithm is derived from the Gauss–Newton algorithm. It is one of the most efficient algorithms used to solve nonlinear fitting. It is thus able to solve our problem in the general case. Nevertheless, the iterative method used here allows us to more clearly distinguish between the two components of the kinetics, binding and reaction, and to offer a graphical interpretation of the complex system.

The method was applied to the determination of the  $K_d$  value of the HA/HAase electrostatic complex from the analysis of the experimental substrate-dependence of the HA hydrolysis catalyzed by HAase. In a first step, the “straight line fitting method” has been used. The first part of the substrate-dependence has been fitted to Eq. (14). The fitting was performed by considering the nine first experimental points. Then, the estimated values were used to rebuild the global substrate-dependence curve. It clearly appeared that the agreement between the curve obtained and the experimental points was not very good. Two other fittings were thus performed with less experimental points, leading to an increase in the  $V_m$  and  $K_m$  values and a decrease in the  $K_d$  value. Diminishing the number of experimental points taken into account also increases the agreement between the rebuilt substrate-dependence curve and the experimental points. In a second step the “global fitting method” was applied to determine the  $V_m$ ,  $K_m$  and  $K_d$  parameters. The values estimated by the “straight line fitting method” seem to tend toward the values estimated by the “global fitting method” when the number of experimental points is diminished. The  $K_d$  was thus estimated at  $2.2 \cdot 10^{-5}$  mol.L<sup>-1</sup>,  $V_m$  to 67 mol.L<sup>-1</sup>.s<sup>-1</sup> and  $K_m$  to  $1.15 \cdot 10^{-3}$  mol.L<sup>-1</sup>.

The  $K_d$  value is consistent with the other  $K_d$  values determined for the binding of HA with proteins such as CD44 [28], LYS [23] or fibroblast growth factor [29] which vary from  $10^{-8}$  to  $10^{-6}$  mol.L<sup>-1</sup>. Nevertheless, the definition of the equilibrium constants found in the literature remains often unclear: is the binding of one molecule of HA with several molecules of protein concerned, or is the binding of one molecule of protein with one fragment of the HA molecule? In the present study, we have clearly considered the latter definition.

To our knowledge, this is the first determination of the dissociation constant of the non-catalytic and non-productive electrostatic complex formed between an enzyme and its polyelectrolytic substrate.

Moreover, we have shown that the inhibition of HAase activity at pH 4 (optimal pH) can be prevented or reversed by addition of proteins able to form similar complexes with HA and so, able to compete with HAase in forming electrostatic complexes with HA. BSA and LYS belong to that class of proteins because their pI is higher than 5 and they are positively charged at pH 4. Addition of such proteins produces the enhancement or the suppression of the HAase activity depending on their concentrations [18–20]. The fact that LYS can enhance HAase activity over a wide pH domain (from 3 to 9) means that LYS can positively compete with HAase to form complexes with HA [21]. That means that the dissociation constant of the HA–HAase complex should be higher than the dissociation constant of the HA–LYS complex [21]. The dissociation constant of the HA–LYS complex being equal to  $10^{-7}$ – $10^{-8}$  M [23], the value obtained here for the HA–HAase complex by using the present model is consistent with our conclusion.

The number of 57 HA carboxyl groups assumed to be involved in the binding of HA with one BTHAase molecule is consistent with the  $n$  value determined by Van Damme et al. [23] for the HA–LYS complex who have reported that 117 molecules of LYS are bound to one HA molecule at pH close to 5. This means that 18 HA carboxyl groups are involved in the binding per LYS molecule which is 4 times smaller than BTHAase ( $M_w$  of LYS =  $14,400 \text{ g.mol}^{-1}$ , and  $M_w$  of BTHAase =  $57,000 \text{ g.mol}^{-1}$ ). However, this only constitutes an approximation because the amino-acid compositions of BTHAase and LYS are different. The primary structures of several HAases are now known [38]: stonefish HAase, *S. horrida* fish HAase, human HAase, mouse HAase, viper HAase, frog HAase, Eastern and Western honey bee HAases. The BTHAase structure does not appear in the protein data bank, but the structure of PH-20 which is the soluble part of BTHAase is known [25]. Data show that PH-20 contains 34 lysine residues, 17 arginine and 6 histidine which are positively charged at pH 5 and mainly located at the surface of the BTHAase molecule [25]. At pH 5, all the positive charges (57) can thus be involved in the binding with 57 carboxyl groups of the HA molecule.

This paper thus shows that it is possible to graphically distinguish between the two phenomena, complexation and reaction, coupled in the functioning of the HA/BTHAase system. This system is an enzymatically catalyzed hydrolysis of a substrate able to electrostatically sequester the enzyme under an inactive form. A similar behavior has been recently observed with bee HAase [39]. This may not be specific to the HA/BTHAase system, but is quite frequent in biology where a great number of polyelectrolytic substrates are metabolized by enzymes in some biological compartments, such as cartilage, where the ionic strength can be much lower than the classic value of  $0.15 \text{ mol.L}^{-1}$  [23]. Polysaccharide/enzyme systems and DNA (or RNA)/enzyme systems may be concerned and it is fundamental to understand that the electrostatic binding between the two biomacromolecules, and especially the order of magnitude of the  $K_d$  constant, can highly control the catalyzed reactions, especially in the ECM where high concentrations of enzymes and polysaccharides exist.

## Acknowledgments

We thank Dr. Viswas Purohit for critical readings of the manuscript. We are grateful to the French Research and Technology Ministry for the fellowship granted to F riel Amar.

## Annex 1

From Eq. (3) and by considering that  $[\text{HAase}_a]/[\text{HAase}]_0$  is close to 1, we may assimilate  $[\text{HAase}_a]$  to  $[\text{HAase}]_0$  in products but not in additions, and write:

$$[\text{HA}_n] = K_d \times [\text{HA}_n - \text{HAase}]/[\text{HAase}]_0 \quad (\text{A1})$$

thanks to Eqs. (4) and (5), we may write:

$$[\text{HA}_n - \text{HAase}] = [\text{HA}_n]_0 - K_d \times [\text{HA}_n - \text{HAase}]/[\text{HAase}]_0 \quad (\text{A2})$$

and thus:

$$[\text{HA}_n]_0 = [\text{HA}_n - \text{HAase}] + K_d \times [\text{HA}_n - \text{HAase}]/[\text{HAase}]_0 \quad (\text{A3})$$

$$[\text{HA}_n]_0 = [\text{HA}_n - \text{HAase}] \times (1 + K_d/[\text{HAase}]_0) \quad (\text{A4})$$

$$[\text{HA}_n]_0 = [\text{HA}_n - \text{HAase}] \times ([\text{HAase}]_0 + K_d)/[\text{HAase}]_0 \quad (\text{A5})$$

$$[\text{HA}_n]_0 \times [\text{HAase}]_0 = [\text{HA}_n - \text{HAase}] \times ([\text{HAase}]_0 + K_d) \quad (\text{A6})$$

$$[\text{HA}_n - \text{HAase}] = [\text{HA}_n]_0 \times [\text{HAase}]_0/([\text{HAase}]_0 + K_d) \quad (\text{A7})$$

replacing  $[\text{HAase}_a]$  by its value in Eq. (4), the binding contribution can thus be expressed by:

$$[\text{HAase}_a]/[\text{HAase}]_0 = ([\text{HAase}]_0 - [\text{HA}_n - \text{HAase}])/[\text{HAase}]_0 \quad (\text{A8})$$

$$[\text{HAase}_a]/[\text{HAase}]_0 = 1 - [\text{HA}_n - \text{HAase}]/[\text{HAase}]_0 \quad (\text{A9})$$

replacing  $[\text{HA}_n - \text{HAase}]$  by its value in Eq. (A7) gives

$$[\text{HAase}_a]/[\text{HAase}]_0 = 1 - [\text{HA}_n]_0/(K_d + [\text{HAase}]_0) \quad (\text{A10})$$

as  $[\text{HA}_\beta]_0 = n \times [\text{HA}_n]_0$ , we may write:

$$[\text{HAase}_a]/[\text{HAase}]_0 = 1 - [\text{HA}_\beta]_0 \times (1/n)/(K_d + [\text{HAase}]_0) \quad (\text{A11})$$

the slope  $s$  of the binding contribution can thus be expressed by:

$$s = -1/n/(K_d + [\text{HAase}]_0). \quad (\text{A12})$$

## References

- [1] C. Schmitt, C. Sanchez, S. Desobry-Banon, J. Hardy, Structure and technofunctional properties of protein–polysaccharide complexes: a review, *Critical Reviews in Food Science* 38 (1998) 689–753.
- [2] C.L. Cooper, P.L. Dubin, A.B. Kayimazer, S. Turksen, Polyelectrolyte–protein complexes, *Current Opinion in Colloid* 10 (2005) 52–78.
- [3] G.F. Palmieri, D. Lauri, S. Martelli, P. Wehrle, Methoxybutyrate microencapsulation by gelatin–acacia complex coacervation, *Drug Development and Industrial Pharmacy* 25 (1999) 399–407.
- [4] Y.F. Wang, J.Y. Gao, P.L. Dubin, Protein separation via polyelectrolyte coacervation: selectivity and efficiency, *Biotechnology Progress* 12 (1996) 356–362.
- [5] P.L. Dubin, J. Gao, K.M. Mattison, Protein purification by selective phase separation with polyelectrolytes, *Separation and Purification Methods* 23 (1994) 1–16.
- [6] M. Erickson, R. Stern, Chain gangs: new aspects of hyaluronan metabolism, *Biochemistry Research International* 2012 (2012) 893947.
- [7] J.B. Catterall, Hyaluronic acid, cell adhesion and metastasis, *Cancer Journal* 8 (1995) 320–324.
- [8] B. Delpech, N. Girard, P. Bertrand, M.N. Courel, C. Chauzy, A. Delpech, Hyaluronan: fundamental principles and applications in cancer, *Journal of Internal Medicine* 242 (1997) 41–48.
- [9] J.F. Kennedy, G.O. Phillips, P.A. Williams, *Hyaluronan*, Woodhead Publishing, Wrexham, Wales, 2002.
- [10] T.C. Laurent, Biochemistry of hyaluronan, *Acta Otolaryngologica. Supplement* (Stockholm) 442 (1987) 7–24.
- [11] P. Rooney, S. Kumar, J. Ponting, M. Wang, The role of hyaluronan in tumour neovascularization, *International Journal of Cancer* 60 (1995) 632–636.
- [12] D.C. West, I.N. Hampson, F. Arnold, S. Kumar, Angiogenesis induced by degradation products of hyaluronic acid, *Science* 228 (1985) 1324–1326.
- [13] D.C. West, S. Kumar, Hyaluronan and angiogenesis, in: D. Evered, J. Whelan (Eds.), *The Biology of Hyaluronan*, vol. 143, John Wiley and Sons, Chichester, 1989, pp. 187–207.
- [14] R. Deed, P. Rooney, P. Kumar, J.D. Norton, J. Smith, A.J. Freemont, S. Kumar, Early response gene signaling is induced by angiogenic oligosaccharides of hyaluronan in endothelial cells. Inhibition by nonangiogenic, high-molecular-weight hyaluronan, *International Journal of Cancer* 71 (1997) 251–256.
- [15] K. Mio, R. Stern, Inhibitors of the hyaluronidases, *Matrix Biology* 21 (2002) 31–37.
- [16] R. Stern, Hyaluronidases in cancer biology, *Seminars in Cancer Biology* 18 (2008) 275–280.

- [17] S. Xu, J. Yamanaka, S. Sato, I. Miyama, M. Yonese, Characteristics of complexes composed of sodium hyaluronate and bovine serum albumin, *Chemical and Pharmaceutical Bulletin* 48 (2000) 779–783.
- [18] H. Lenormand, F. Tranchepain, B. Deschrevel, J.C. Vincent, The hyaluronan–protein complexes at low ionic strength: how the hyaluronidase activity is controlled by the bovine serum albumin, *Matrix Biology* 28 (2009) 365–372.
- [19] H. Lenormand, B. Deschrevel, F. Tranchepain, J.C. Vincent, Characterisation of hyaluronan–protein electrostatic complexes and their role in the control of the hyaluronidase activity, *Biopolymers* 89 (2008) 1088–1103.
- [20] B. Deschrevel, H. Lenormand, F. Tranchepain, N. Levasseur, T. Astériou, J.C. Vincent, Hyaluronidase activity is modulated by complexing with various polyelectrolytes including hyaluronan, *Matrix Biology* 27 (2008) 242–253.
- [21] H. Lenormand, B. Deschrevel, J.C. Vincent, pH effects on the hyaluronan hydrolysis catalysed by hyaluronidase in the presence of proteins: part I. Dual aspect of the pH-dependence, *Matrix Biology* (2010) 330–337.
- [22] H. Lenormand, J.C. Vincent, pH effects on the hyaluronan hydrolysis catalysed by hyaluronidase in the presence of proteins: part II. The electrostatic hyaluronan–protein complexes, *Carbohydrate Polymers* 85 (2011) 303–311.
- [23] M.P.I. Van Damme, J.M. Moss, W.H. Murphy, B.N. Preston, Binding properties of glycosaminoglycans to lysozyme – effect of salt and molecular weight, *Archives of Biochemistry and Biophysics* 310 (1994) 16–24.
- [24] I. Morfin, E. Buhler, F. Cousin, I. Grillo, F. Boué, Rodlike complexes of a polyelectrolyte (hyaluronan) and a protein (lysozyme) observed by SANS, *Biomacromolecules* 12 (2011) 859–870.
- [25] H. Lenormand, F. Amar-Bacoup, J.C. Vincent, pH effects on the hyaluronan hydrolysis catalysed by hyaluronidase in the presence of proteins: part III. The electrostatic non-specific hyaluronan–hyaluronidase complex, *Carbohydrate Polymers* 86 (2011) 1491–1500.
- [26] J.C. Vincent, H. Lenormand, How hyaluronan–protein complexes modulate the hyaluronidase activity: the model, *Biophysical Chemistry* 145 (2009) 126–134.
- [27] C. Maingonnat, R. Victor, P. Bertrand, M.N. Courel, R. Maunoury, B. Delpech, Activation and inhibition of human cancer cell hyaluronidase by proteins, *Analytical Biochemistry* 268 (1999) 30–34.
- [28] T.P. Skelton, C. Zeng, A. Nocks, I. Stamenkovic, Glycosylation provides both stimulatory and inhibitory effects on cell surface and soluble CD44 binding to hyaluronan, *The Journal of Cell Biology* 140 (1998) 431–446.
- [29] I. Freeman, A. Kedem, S. Cohen, The effect of sulfation of alginate hydrogels on the specific binding and controlled release of heparin-binding proteins, *Biomaterials* 29 (2008) 3260–3268.
- [30] S.J. Frost, R.H. Raja, P.H. Weigel, Characterization of an intracellular hyaluronic acid binding site in isolated rat hepatocytes, *Biochemistry* 29 (1990) 10425–10432.
- [31] J.C. Vincent, T. Astériou, B. Deschrevel, Kinetics of hyaluronan hydrolysis catalysed by hyaluronidase. Determination of the initial reaction rate and the kinetic parameters, *Journal of Biological Physics and Chemist* 3 (2003) 35–44.
- [32] H. Lenormand, B. Deschrevel, J.C. Vincent, How electrostatic interactions can change the kinetic behaviour of a Michaelis–Menten type enzyme. Application to the hyaluronane / hyaluronidase system, *Journal of Biological Physics and Chemist* 7 (2007) 129–134.
- [33] K. Meyer, Hyaluronidases, in: 3rd ed., P.D. Boyer (Ed.), *The Enzymes*, vol. 5, 1971, pp. 307–320.
- [34] J. Reissig, J. Strominger, J. Leloir, A modified colorimetric method for the estimation of N-acetylamino sugars, *Journal of Biological Chemistry* 217 (1955) 959–966.
- [35] T. Astériou, B. Deschrevel, B. Delpech, P. Bertrand, F. Bultelle, C. Merai, J.C. Vincent, An improved assay for the N-acetyl-D-glucosamine reducing ends in the presence of proteins, *Analytical Biochemistry* 293 (2001) 53–59.
- [36] T. Astériou, J.C. Vincent, F. Tranchepain, B. Deschrevel, Inhibition of hyaluronan hydrolysis catalysed by hyaluronidase at high substrate concentration and low ionic strength, *Matrix Biology* 25 (2006) 166–174.
- [37] D. Marquardt, An algorithm for least-squares estimation of nonlinear parameters, *SIAM Journal on Applied Mathematics* 11 (1963) 431–441.
- [38] M. Madokoro, A. Ueda, A. Kiriake, K. Shiomi, Properties and cDNA cloning of a hyaluronidase from the stonefish *Synanceia verrucosa* venom, *Toxicon* 58 (2011) 285–292.
- [39] A. Iliás, K. Liliom, B. Greiderer-Kleinlercher, S. Reitingner, G. Lepperdinger, Unbinding of hyaluronan accelerates the enzymatic activity of bee hyaluronidase, *Journal of Biological Chemistry* 286 (2011) 35699–35707.